Fluid flow in channels between two gas turbines and heat recovery steam generator – a theoretical investigation

H. WALTER, C. DOBIAS, F. HOLZLEITHNER
Institute for Energy Systems and Thermodynamics
Vienna University of Technology
Getreidemarkt 9 / 302, 1060 Vienna
AUSTRIA
heimo.walter@tuwien.ac.at http://www.tuwien.ac.at/iet

R. HOFMANN
BERTSCHenergy, Kessel- und Energietechnik Apparatebau,
Josef Bertsch Ges.m.b.H. & Co
Herrengasse 23, A-6700 Bludenz
AUSTRIA
rene.hofmann@bertsch.at http://www.bertsch.at

Abstract: - The paper present the results of a study for a special configuration of a combined cycle power plant. In this plant two gas turbines are installed to feed one Heat Recovery Steam Generator (HRSG). The flue gas flow in the channels between the two gas turbines and the HRSG was analyzed to get a more homogenous flow distribution in front of the first heating surface of the HRSG which is arranged downstream of the gas turbines. In the study a particular attention was placed at the operation conditions where only one gas turbine is in operation.
The results of the investigation have shown that the measures with a higher possibility to get a homogenous flow distribution in front of the first tube bank arranged downstream of the gas turbine have also a higher pressure loss and in last consequence they are linked with a higher loss of gas turbine power respectively a lower efficiency of the combined cycle. The study has also shown that a larger merging area for the flue gas arranged between the merging point of the two flue gas ducts and the entrance into the HRSG results in a more even flow distribution.

Key-Words: - Numerical simulation, Flue gas channel, Heat recovery steam generator, Channel optimization, Flow distribution

1 Introduction

The growing industry and world population results in an increased demand on energy and as a consequence of this energy consumption also in a increased emission of greenhouse gases. In view of the uncertainties related to global warming and the availability of primary energy sources, there is a requirement to reduce CO_2 emissions and the energy consumption. Apart from saving of energy an important part can be provided by an increased use of waste heat of industrial applications.

In the energy and chemical industry there are many applications where waste heat can be used by another process. For example the exhaust flue gas of a gas turbine or of a furnace blower can be used in a Heat Recovery Steam Generator (HRSG) to produce steam for another process and/or to produce electricity or for district heating; the waste heat of a gas engine can be used by a downstream arranged Organic Rankine Cycle (ORC) to produce additional electricity and so on.

In e.g. a coal fired power plant the flue gas allocates the heat flux at high temperature whose exergy can be used only in an inadequate way. Because the upper temperature level of the superheated steam with approx. 550 °C is much lower compared to the flue gas temperature in the combustion chamber of the coal fired power plant with approx. 1500 °C. An increase of the steam parameters cannot be done due to the economic choice as well as the strength of the material used. Therefore the high loss of exergy at the heat transfer in the steam generator should be avoided.

The provided exergy at high temperature can be used in another and better way in the combustion chamber of a turbo-machinery followed by an expansion of the flue gas in an expander where electricity can be produced. The high exergy of the gas turbine exhaust flue gas can be used in a downstream arranged Rankine cycle to produce steam for another process and/or electricity.

The combination of the gas turbine and the Rankine cycle is called combined cycle, where the waste heat of the gas turbine cycle is used in a heat recovery steam generator in a most efficient way to increase the thermal efficiency of the single gas turbine cycle. Heavy duty natural gas fired gas turbines in combination with heat recovery steam generators and steam turbines represent the state of the art of this approach [1]. The efficiency of the latest combined power plants are very high. For example the RWE combined cycle power plant Emsland, unit D in Lingen, Germany with an Alstom gas turbine GT 26 has achieved an overall efficiency for the plant of 59.2% [2] or the Eon-power plant Irshing, unit 4 erected in Irshing, Germany with a Siemens gas turbine SGT5 8000 H will achieve a efficiency with the combined power plant of > 60% [3] to [6].

In this paper the exhaust flue gas flow in the channels between two gas turbines and one heat recovery steam generator arranged downstream of the gas turbines was analysed with the help of the commercial CFD-Code FLUENT 6.3. Based on the limited area for erecting the HRSG the merging point of the channels is arranged very close to the flue gas entrance of the HRSG (see figure1 and 2).

Under normal operation conditions the natural circulation HRSG is feed by the two gas turbines, which results in a relatively even flow distribution in front of the first heating surface of the HRSG. But in some cases only one of the two gas turbines is in operation. This results to an uneven incident flow in front of the first tube bank of the HRSG (super-heater SH1) which should be prevented.

A non-uniform flue gas flow distribution in the tube banks of a natural circulation steam generator can result in an unstable behaviour of the working medium in the evaporator of this boiler (see e.g. [7] – [11]). In this case reverse flow and/or flow stagnation can occur especially under hot start-up or heavy load changes. The experience shows, that these operation modes are the most critical.

First results of a numerical investigation to get a more homogeneous flow distribution in front of the first heating surface of the HRSG arranged downstream of the flue gas duct will be presented.

2 Description of the analysed channel and boiler

In figure 1 the analysed channels as well as the natural circulation vertical type HRSG, which is arranged downstream of two natural gas fired gas turbines, is presented. Every gas turbine has a power output of 53 MW, a flue gas mass flow of 130 kg/s with a turbine exit temperature of approx. 550 °C. The figure shows the boiler included stack, diverter with bypass stack, field devices, steel structure and pipe work inside the boiler house. Due to standardization of the gas turbines of the different manufacturers the HRSG have to be optimized to achieve optimum thermal efficiencies. This drum type boiler is a natural circulation system with a vertical flue gas path in top supported design and multi-pressure systems. The present boiler design includes a high and a low pressure system with the steam parameters shown in table 1. The super-heater temperature is controlled using spray attemporators arranged between the individual super-heater stages.

Fig. 1: Sketch of the analysed steam generator [12]

In figure 1 the analysed channels arranged between the two gas turbines and the HRSG are also presented. The dimensions of the channels can be seen in figure 2. Downstream of the gas turbines the channel changes from a circular to a rectangular duct. Both channels merge in front of the HRSG (see also figure 2). After the merging point of the two flue gas ducts the gas turbine exhaust gas changes the flow direction from horizontal to vertical direction. After the change of the flow direction the flue gas enters the first heating surface (super heater tube bank 1) at the bottom of the HRSG. The gas turbine exhaust flue gas leaves the HRSG at the top through the chimney.

Table 1 presents the main technical specifications of the HRSG under investigation.

TABLE 1
TECHNICAL DATA OF THE HRSG [12]

Specification	Quantity
Maximum continuous rating (high pressure)	130 t/h
Maximum continuous rating (low pressure)	29 t/h
super-heated steam pressure (high pressure)	121 bar
super-heated steam pressure (low pressure)	4.2 bar
super-heated steam temperature (high pressure)	515 °C
super-heated steam temperature (low pressure)	170 °C

3 Mathematical analysis

3.1 Governing equation of the fluid flow

For the numerical analysis a three dimensional computational domain is constructed with the help of GAMBIT (FLUENT [13]) for modelling the channel and a part of the flue gas pass of the HRSG. The model consists of the two flue gas ducts and the lower part of the vertical type HRSG including three super-heater tube banks. Super-heater 1 (SH1) is arranged at the inlet of the flue gas into the HRSG and super-heater 2 (SH2) and 3 (SH3) are arranged downstream of super-heater 1 (see figure 3).

The main dimensions of the analysed channels as well as of the simulated part of the HRSG are presented in the isometric sketch of figure 2. In this figure it can be seen that the merging point of the channels is arranged very close to the entrance region of the HRSG. This was a result of the limited area for erecting the HRSG. Therefore only a very short calming section is available for the merging flue gas.

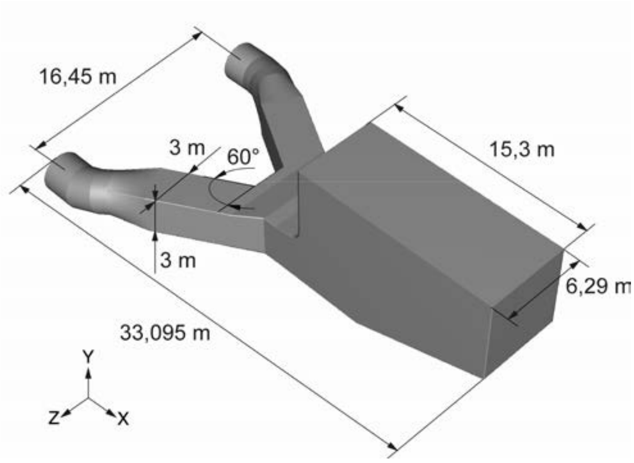

Fig. 2: Main dimensions of channels and HRSG used for calculations

The discretization of the partial differential equations for the conservation laws is done in Fluent [13] with the aid of the finite-volume-method. The pressure-velocity coupling and overall solution procedure used in this study is based on the pressure correction algorithm SIMPLE (Semi Implicit Method for Pressure Linked Equations) [14]. For the convective term the Second Order UPWIND scheme is used. This gives a good accuracy of the solution.

The steady state computations of the fluid flow in the channels and HRSG are done for three dimensions. The governing equations for the fluid flow are:

Continuity equation:

$$\frac{\partial \rho}{\partial t} + \frac{\partial(\rho u_i)}{\partial x_i} = 0 \qquad (1)$$

Momentum equation:

$$\frac{\partial(\rho u_i)}{\partial t} + \frac{\partial(\rho u_i u_i)}{\partial x_i} = -\frac{\partial p}{\partial x_i} + \frac{\partial \tau_{ij}}{\partial x_i} + \rho g_i \qquad (2)$$

Energy equation:

$$\frac{\partial(\rho h_i)}{\partial t} + \frac{\partial(\rho u_i h_i)}{\partial x_i} = \frac{\partial p}{\partial t} + \tau_{ij}\frac{\partial u_j}{\partial x_i} + u_i \frac{\partial p}{\partial x_i} \qquad (3)$$

Here u_i denotes the velocity component in i direction, t the time, ρ the fluid density and x_i the Cartesian coordinate. p is the pressure, g_j is the gravitational acceleration, h is the specific enthalpy.

τ_{ij} stands for the viscous stress tensor and can be expressed for a Newtonian fluid as:

$$\tau_{ij} = \mu\left(\frac{\partial u_i}{\partial x_j} + \frac{\partial u_j}{\partial x_i}\right) - \frac{2}{3}\delta_{ij}\frac{\partial u_k}{\partial x_k} \quad (4)$$

with the dynamic viscosity μ and the Kronecker delta δ_{ij}.

3.2 Turbulence modelling

For modelling the turbulence the realizable k-ε model with the standard wall functions was chosen during the simulation. The main differences between the realizable and standard k-ε model is given in the turbulent viscosity μ_t and the new equation for calculating the turbulent rate of dissipation ε, which is derived from the exact equation for the transport of the mean-square vorticity fluctuation [13].

The partial differential equations in conservative form for the realizable k-ε model is described in detail in [13] and can be seen as follow:

Turbulent kinetic equation:

$$\frac{\partial}{\partial x_i}(\rho k u_i) = \frac{\partial}{\partial x_i}\left[\left(\mu + \frac{\mu_t}{\sigma_k}\right)\frac{\partial k}{\partial x_i}\right] + G_k + G_b - \rho\varepsilon - Y_M \quad (5)$$

which is the same as for the standard k-ε model.

Turbulent kinetic dissipation equation:

$$\frac{\partial}{\partial x_i}(\rho \varepsilon u_i) = \frac{\partial}{\partial x_i}\left[\left(\mu + \frac{\mu_t}{\sigma_\varepsilon}\right)\frac{\partial \varepsilon}{\partial x_i}\right] + \rho C_1 S\varepsilon - \rho C_2 \frac{\varepsilon^2}{k + \sqrt{\nu\varepsilon}} + C_{1\varepsilon}\frac{\varepsilon}{k}C_{3\varepsilon}G_b \quad (6)$$

with

$$C_1 = \max\left[0{,}43; \frac{\eta}{\eta + 5}\right]; \quad \eta = S\frac{k}{\varepsilon}; \quad S = \sqrt{2S_{ij}S_{ij}}$$

In these equations k represents the turbulent kinetic energy, ν the kinetic viscosity, G_k the generation of turbulence kinetic energy due to the mean velocity gradients, G_b the generation of turbulence kinetic energy due to the buoyancy, σ_k and σ_ε the turbulent Prandtl-number for k and ε, respectively. The contribution of the fluctuating dilatation in compressible turbulence to the overall dissipation rate is represented by Y_M and S is the modulus of the mean rate-of-strain tensor.

The turbulent viscosity is given with:

$$\mu_t = \rho C_\mu \frac{k^2}{\varepsilon} \quad (7)$$

In comparison to the standard k-ε model the coefficient C_μ is not constant in the realizable k-ε model. C_μ is a function of the mean strain and rotation rates, the angular velocity of the system rotation, and the turbulent field.

For the realizable k-ε turbulence model the suggested default values of FLUENT for the model constants $C_{1\varepsilon}$ = 1.44; C_2 = 1.9, σ_k = 1, and σ_ε = 1.2 are used.

For the steady state calculations the time depending term in the equations (1) to (3) as well as (5) and (6) is identical zero.

3.3 Boundary conditions for the simulation

For the numerical simulation of the fluid flow in the channels between the gas turbines and the HRSG boundary conditions are necessary. At the channel inlet (= gas turbine outlet; see figure 2) the velocity distribution of the gas turbine exhaust flue gas for the three coordinate directions x, y and z as well as the gas turbine outlet temperature of the fluid with 550 °C are given. Both gas turbines have the swirl into the same direction. The fluid pressure at the outlet of the computational domain (downstream of the third super-heater) is known from a steady state design calculation of the boiler with 102300 Pa.

The heating surfaces of the three super-heater tube banks included in the computational domain are modelled as porous medium to consider their influence on the flue gas flow. This modelling technique for tube banks in a flue gas pass of a boiler is an approved method and was used e.g. in [16] to [19]. The pressure drop across the different tube banks in the convective pass of the boiler are known from the steady state design calculation. For the numerical calculations in FLUENT the pressure drop over the single tube bank is converted to a velocity dependent pressure loss coefficient per m porous media. The porosity of the porous media used for the simulations was 0.7. The value for the porosity was calculated from the geometrical data of the different tube banks, e.g. longitudinal and transversal pitch, number of passes, and so on.

The heat absorption of the different heating surfaces is modelled as a sink term in the corresponding porous medium to model the flue gas temperature drop. The values for the absorbed heat per volume unit for the different super-heater tube banks and operation conditions are presented in Table 2.

The values for the heat fluxes, which are also known from the design calculations, are for an operation load of the gas turbines of 100%. The simulations where only one gas turbine is under operation (GT 1 in figure 3) are done in such a way that always the same gas turbine was set out of operation. In these cases the inlet boundary conditions for the gas turbine out of operation are replaced by a wall (no backward flow into the gas turbine out of operation was possible).

TABLE 2
HEAT FLUX FROM THE FLUE GAS TO THE HEATING SURFACES

Heating Surface	2 gas turbines in operation	1 gas turbine in operation
super-heater 1	444.6 kW/m^3	223.4 kW/m^3
super-heater 2	297.1 kW/m^3	195.0 kW/m^3
super-heater 3	228.8 kW/m^3	178.7 kW/m^3

Based on the high excess air at the combustion of the fuel in the gas turbine combustor for the exhaust flue gas a simplification for the numerical simulations was made in that form that the thermodynamic properties of air are used. All walls surrounding the channels and the HRSG are modelled as adiabatic walls.

4 Analysed channel configurations

For the numerical simulation of the fluid flow in the channels different configurations are analysed to get a more homogeneous flow distribution in front of the first heating surface of the HRSG (see figure 3) for the case that only gas turbine 1 is in operation (worst case operation mode).

The fluid flow in a channel can be influenced with inserts e.g. perforated plates or baffle plates. But it is also well known that every installation of inserts into a flue gas duct results in an increase of the pressure drop. A consequence of an increasing pressure drop downstream of a gas turbine is that the efficiency of the gas turbine decreases. As a rule of thumb can be seen that a increase of the pressure drop of 1 mbar results in a decreases of gas turbine efficiency of approx. 0.05% points [15]. Thus the additional pressure drop caused by channel inserts must be small as possible.

In the study presented in this paper perforated plates as well as baffle plates are installed into the flow channel. The following cases are analysed:

1) No inserts are installed into the flue gas channel (reference model).
2) Baffle plates installed in the center of the flue gas channel close to the merging point and also close to the gas turbine outlet; see figure 6.
3) Perforated plates installed close to the merging point and the inlet of the HRSG with a porosity of 0.65 (perforated plates - case 1).
4) The same arrangement as in case 3 but with a porosity of 0.8 (perforated plates - case 2).
5) Increase of the channel length between the merging point of the two flue gas ducts and the boiler by 1.5 m and including of two perforated plates close to the merging point and the inlet of the HRSG with a porosity of 0.65 (perforated plates - case 3).
6) Increase of the channel length between the merging point of the two flue gas ducts and the boiler by 1.5 m and including of two perforated plates close to the merging point and the inlet of the HRSG with a porosity of 0.8 (perforated plates - case 4).

The pressure loss coefficient for the perforated plates used in cases 3 to 6 are calculated with the help of [20].

5 Simulation results

The velocity and temperature plots for all figures presented in this paper represent the same section planes (see figure 3 and 5). For the presentation of the velocity two horizontal planes are used. The first plane is arranged at the middle of the flue gas channel while the second plane is arranged in front of the first tube bank. For a better comparison a non-dimensional form for the results of the flue gas velocity are used. In all figures the same reference velocity was used.

For the presentation of the temperature distribution four vertical planes are used. The arrangement of these planes can be seen in figure 5.

5.1 Reference model

Fig. 3 shows the velocity distribution of the flue gas in the planes 1 and 2 for the case that both gas turbines are in operation. It can be seen in figure 3 that the incident flow in front of the first tube bank (SH1) of the HRSG is unsymmetrical although both gas turbines are in operation. As a result of this behaviour on the left side of the HRSG inlet a vortex area (blue coloured) of the flue gas has been build. Based on the momentum exchange between the fluid streams leaving the single flue duct, the exhaust flue gas of GT1 is diverted in direction to the left side of the HRSG. This results in a smaller vortex area during the operation with two gas turbines. The development of this uneven flow distribution at the inlet region of the HRSG is a result of the swirl flow at both gas turbines outlet.

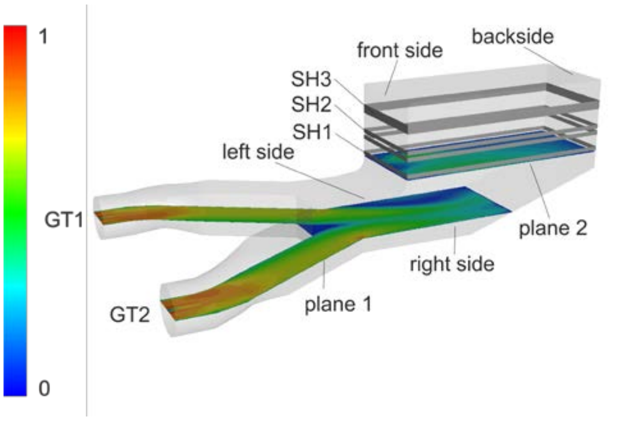

Fig. 3: Velocity magnitudes in two planes of the channel without inserts (GT1 and GT2 in operation)

Plane 2 is arranged close to the inlet of the flue gas flow into SH1. The fluid flow at the left and at the backside of the HRSG is much lower compared to the velocity at the right and at the front side (entrance into the HRSG) of the HRSG. The fluid structure in plane 2 is very similar to that in plane 1.

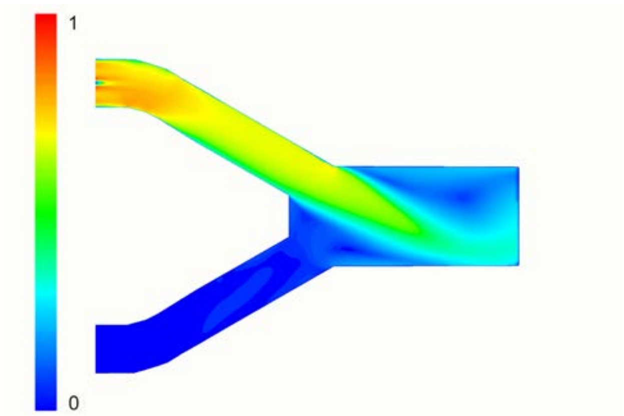

Fig. 4: Velocity magnitudes at plane 1 (only GT 1 is in operation)

The velocity magnitude for the fluid flow during the operation with one gas turbine is presented in figure 4. The figure shows an expected result. The unhindered inflow of the fluid into the base frame of the HRSG results in a great vortex area and in an extreme uneven fluid distribution.

The temperature distribution of the flue gas in different section planes (planes 3 to 6) is presented in figure 5 for the case that only GT1 is in operation. The non-homogenous flow distribution at the inlet of the HRSG results in an unbalanced temperature profile over the tube banks. At the front side the uneven temperature streams are stronger developed compared to the backside of the HRSG. This is a result of the higher fluid mass flow at the right front side of the HRSG.

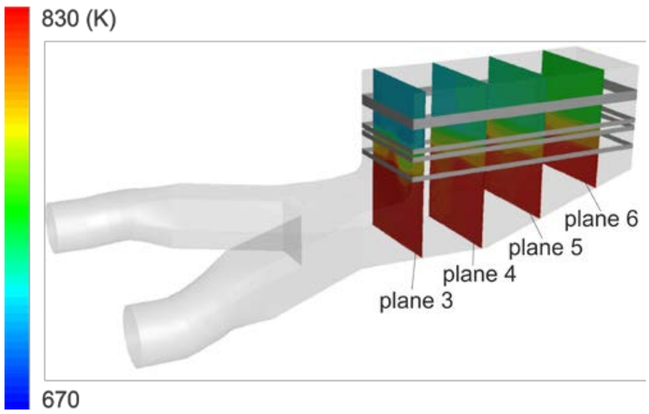

Fig. 5: Temperature distribution of the flue gas (only GT 1 is in operation)

The temperature distribution of the flue gas for the case where both gas turbines are in operation is similar to the situation presented in figure 8a. Therefore no additional figure will be presented. In this case the flow is more homogenous and therefore the temperature distribution in the tube banks is stratified according to the tube banks.

It should be mentioned at this point, that the temperature distribution of the flue gas upstream of super heater 1 (SH1) is only qualitative. The reason is based on the model for the heat exchangers. As mentioned above the tube banks are modelled as a porous medium with an constant heat absorption per volume (see table 2). This results in the circumstance that the heat loss of the flue gas is independent from the temperature difference between the surface temperature of the tubes of the tube bank and the flue gas.

5.2 Baffle plates

Fig. 6 shows the velocity distribution of the flue gas in the planes 1 and 2 for the case that both gas turbines are in operation. The figure presents also the design and the arrangement of the baffle plates included in the flue gas duct. Compared with the reference model in figure 3 it can be seen that the baffle plats influences the fluid flow only in a small measure. Therefore the vortex area at the left side of the HRSG (see mid-plane 1) further exist but with a smaller dimension. The flow distribution at the inlet of the HRSG (plane 2) shows only a minor improvement.

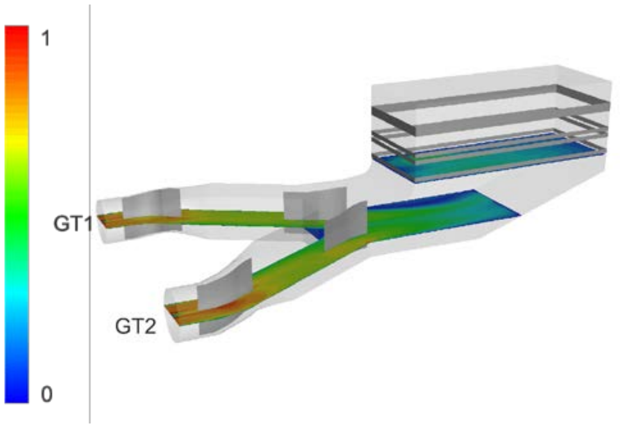

Fig. 6: Velocity magnitudes in two planes of the channel (GT1 and GT2 in operation)

The same behaviour as in the reference model can be seen during the operation with one gas turbine (figure 7). Also in this case the influence of the baffle plates on the fluid characteristic is compared to the reference model (figure 4) small. The fluid stream is deflected by the baffle plates in direction to the middle of the HRSG, but not in a sufficient way.

If we make a look at the flue gas temperature distribution in the flue gas pass of the HRSG then we get a confirmation of this statement.

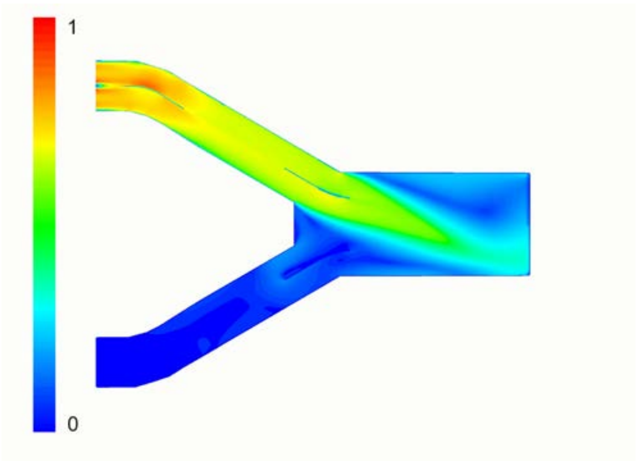

Fig. 7: Velocity magnitudes at plane 1 (GT 1 in operation)

Fig. 8 shows the temperature distribution of the flue gas passing the tube banks of the HRSG. In figure 8a both gas turbines GT1 and GT2 and in figure 8b only GT1 is in operation. It is no improvement given compared to the results of the reference model. Fig. 8b shows also that on the left front side of the HRSG a higher flue gas mass flow stream enters the HRSG. Therefore the downstream arranged tube banks are passed by a flue gas stream with a higher temperature while at the right front side the flue gas stream is cooler. In direction to the backside of the HRSG the uneven temperature profile along the different tube banks reduces.

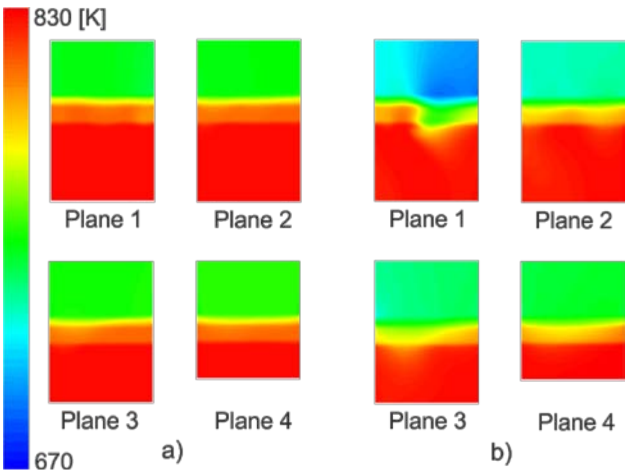

Fig. 8: Vertical temperature distribution of the flue gas a) both gas turbines are in operation b) only GT1 is in operation

5.2 Perforated plates – case 1

Another well-known method to get a more homogenous flow distribution is the installation of perforated plates into a flow duct. Based on the small distance between the merging point of the two channels and the HRSG inlet three perforated plates are installed into the flow channel. The position of the plates is shown in figure 9. Every perforated plate has the same porosity of 0.65 which is equivalent to a pressure loss coefficient of approx. 1.41.

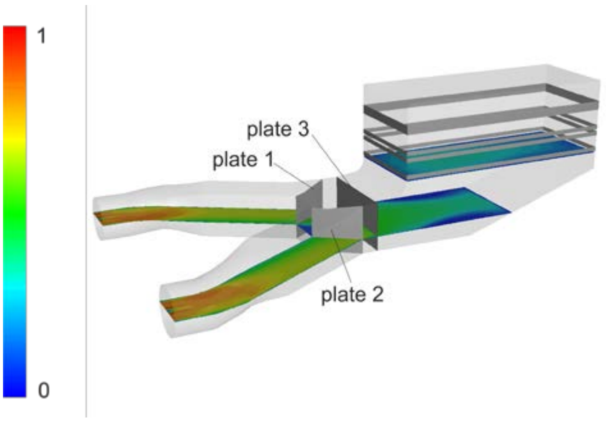

Fig. 9: Velocity magnitudes in two planes of the channel with inserted perforated plates (GT1 and GT2 in operation)

Fig. 9 shows the velocity distribution of the flue gas in the planes 1 and 2 for the case that both gas turbines are in operation. A comparison with the reference model shows that a significant enhancement for the flow in front of SH1 is given (see also figure 10). After passing of plate 3 the fluid enters the base frame of the HRSG with a very homogenous and symmetrical flow distribution over the width of the HRSG. However, figure 10 shows also that on every side wall of the HRSG a smaller vortex with a very low velocity has been formed. This is a result of the flow deflection at the inclined base frame and the wall at the backside of the HRSG. But the influence of both vortices on the velocity distribution of the flue gas in the tube banks of the HRSG is negligibly small.

The temperature distribution of the flue gas along the tube banks is not presented for this analysed case, but it is similar to that presented in figure 8a.

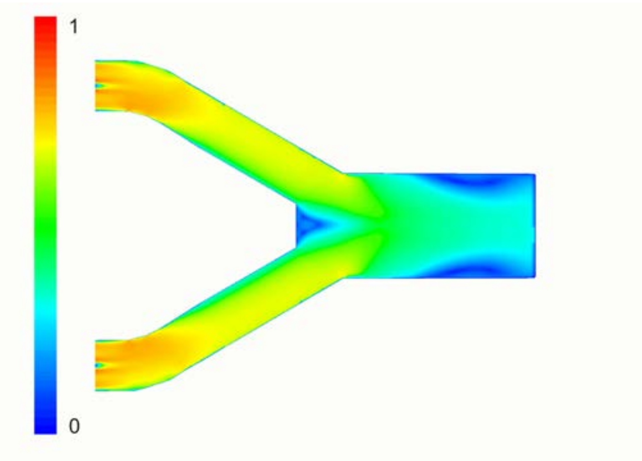

Fig. 10: Velocity magnitudes in plane 1 of the channel with inserted perforated plates (GT1 and GT2 in operation)

Fig. 11 shows the simulation results for the case where only GT1 is in operation. It can be seen clearly that also in this case the flow distribution is more homogenous compared to the reference model.

The decrease of the unbalance in the fluid flow is most significant. The fluid velocity is over a wider range of the base frame of the HRSG approximately the same. A smaller area with a reverse flow of the fluid can be seen in figure 11 represented by the small blue stripe at the left side of the HRSG wall.

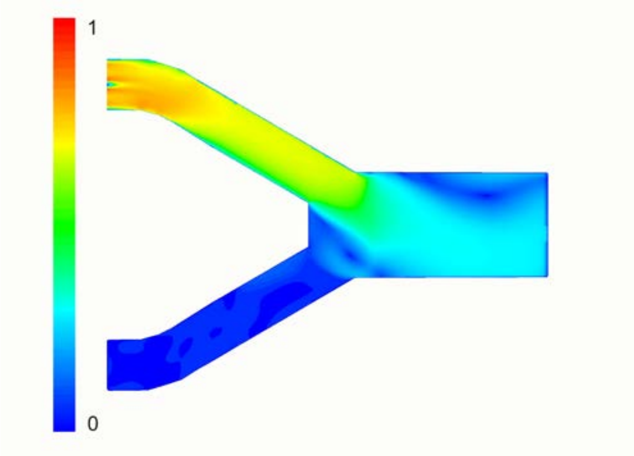

Fig. 11: Velocity magnitudes at plane 1 with inserted perforated plates (GT 1 in operation)

5.3 Perforated plates – case 2

The second analysed case with perforated plates deals with the same inserts in the flue gas duct as presented in section 5.2. The only difference between the two cases is the porosity of perforated plates. The porosity was changed from 0.65 to 0.8. This results in a pressure loss coefficient of approx. 0.42 according to [20].

Fig. 12 shows the velocity distribution simulated under the new conditions for both gas turbines in operation which is unsurprising. The higher porosity of the plates results in a more uneven fluid flow. Compared to the result presented in figure 10, where the flow is very homogenous after leaving the plates, tends the flow under the current investigated conditions in direction to the reference model (see figure 3).

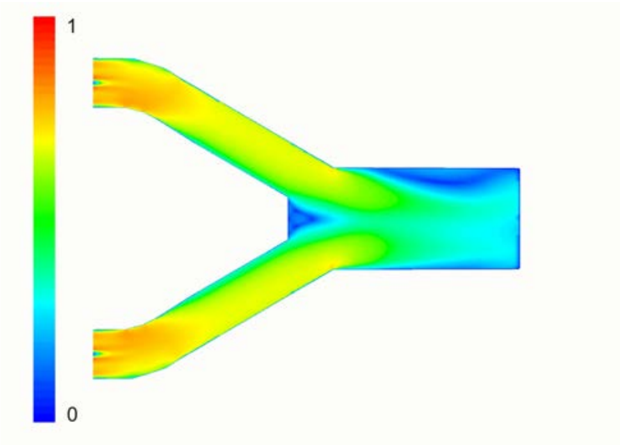

Fig. 12: Velocity magnitudes in plane 1 of the channel with inserted perforated plates (GT1 and GT2 in operation)

As it can be seen in figure 12 the flow leans to the right side wall of the HRSG and the vortex area starts to grow. But in summery the distribution of the flow is more preferable compared to that of the reference model.

The temperature distribution for the flue gas in the tube banks, which are not presented in this paper, is similar to that presented in figure 8a.

Fig. 13 shows the simulation results for the velocity under the condition that only GT1 is in operation. As discussed above the velocity distribution is also in this case more uneven compared to the results presented in figure 11 for the higher value of the porosity. In contrast to the result presented in figure 11 a more closed fluid stream has been formed which results in a greater vortex area with a smaller velocity of the fluid at the left side of the HRSG.

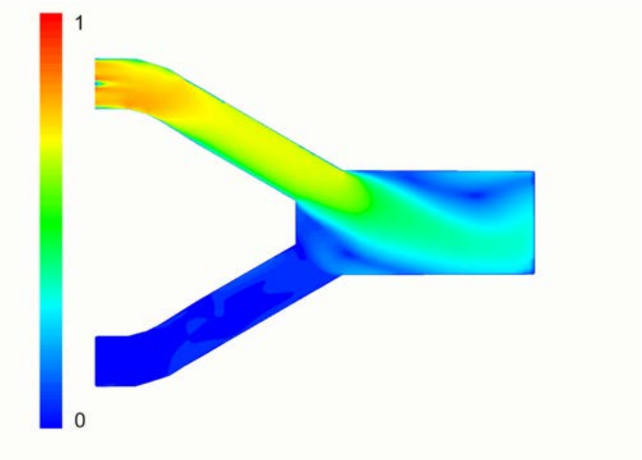

Fig. 13: Velocity magnitudes at plane 1 with inserted perforated plates (GT 1 in operation)

This can be seen also in the temperature distribution of the fluid along the flue gas pass. In figure 14 a comparison of the temperature distribution of the flue gas along the tube banks for the analysed configurations with the perforated plate cases 1 and 2 are presented. The figure shows that a more even temperature profile along the flue gas pass is given under the conditions of perforated plates with higher porosity. Fig. 14 shows also that a higher flue gas mass flow is given at the right side while the simulations with the baffle plates have shown the higher mass flow at the left side of the HRSG.

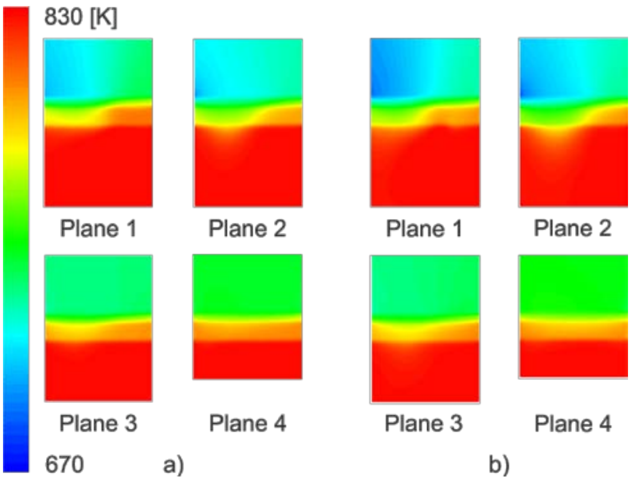

Fig. 14: Vertical temperature distribution of the flue gas (GT1 is in operation) a) perforated plates – case 1 and b) perforated plates – case 2

The following two analysed cases with perforated plates included in the flue gas duct have a differing channel geometry compared to all other cases (reference model and baffle plates as well as perforated plates cases 1 and 2) presented above.

In the new arrangement the position of the perforated plates as well as a new geometry for the mixing zone between the merging point of the two flue gas ducts arranged downstream of the gas turbines and the HRSG are analysed. In these analysed cases the mixing zone for the flue gas was increased by 1.5 m (total length of the computational domain is changed from 33,095 m to 34,595 m. Compare with figure 2). All other geometrical dimensions are retained constant. This investigation was done to clarify the flow behaviour in front of the HRSG in case of a larger available mixing zone.

5.4 Perforated plates – case 3

Fig. 15 shows the new arrangement of the computational domain as well as the new position of the perforated plates. Every perforated plate has the same porosity of 0.65 which is equivalent to a pressure loss coefficient of approx. 1.41. As a result of the new geometry only two perforated plates must be used. These two plates can be arranged parallel in the mixing zone of the flue gas channel.

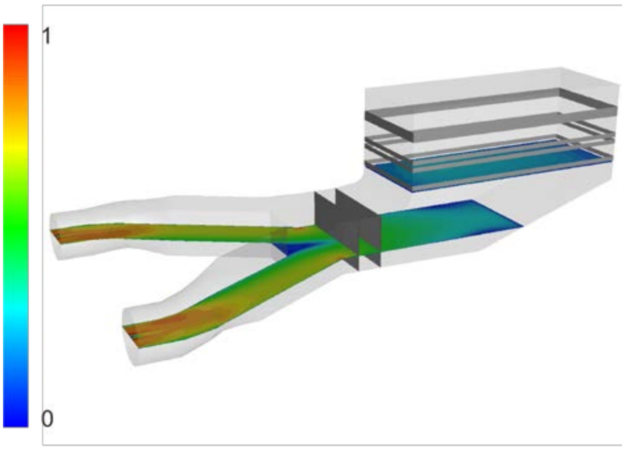

Fig. 15: Velocity magnitudes in two planes of the channel with inserted perforated plates (GT1 and GT2 in operation)

Fig. 16 shows the velocity distribution of the flue gas in plane 1 for the case that both gas turbines are in operation. It can be seen, that the flue gas distribution in the base frame of the HRSG (upstream of the first heating surface SH1) is very homogeneous. A comparison with all other analysed cases presented above shows that this arrangement provides the best results.

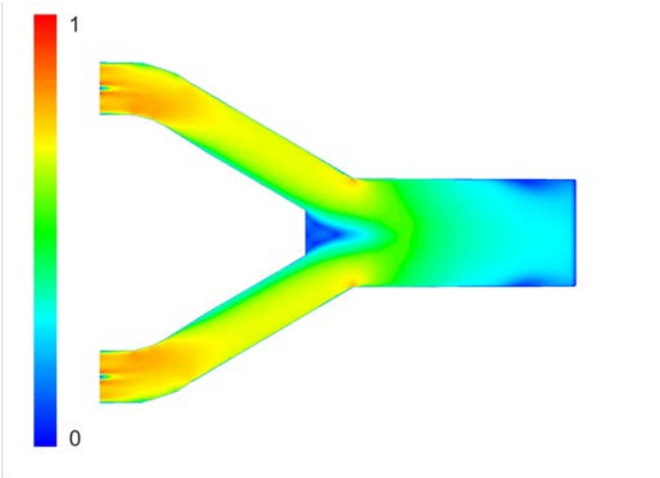

Fig. 16: Velocity magnitudes at plane 1 with inserted perforated plates (GT1 and GT2 in operation)

However, figure 16 shows also that on both side walls of the HRSG a more or less negligible vortex with a very low velocity has been formed. These very small vortex areas are disappeared in plane 2 (not presented in this paper), which is arranged directly in front of the super-heater 1.

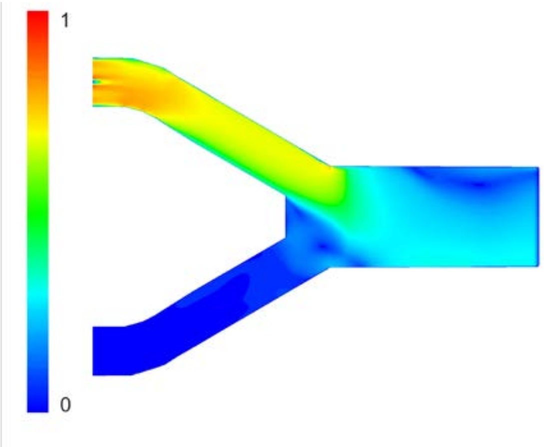

Fig. 17: Velocity magnitudes at plane 1 with inserted perforated plates (GT1 in operation)

In figure 17 the velocity distribution of the flue gas in plane 1 for the case that only gas turbine 1 is in operation is presented. The figure shows the same tendency to a more even flow distribution of the flue gas. The vortex area at the left side of the HRSG is the smallest in case of an operation mode with one gas turbine. Therefore the incident flow in front of the first heating surface SH1 is more favourable compared to the other presented cases with only gas turbine GT 1 in operation.

5.5 Perforated plates – case 4

Fig. 18 shows the velocity magnitudes of the flue gas inside the new channel geometry for the operation mode with two gas turbines. The numerical simulation was done for perforated plates with a porosity of 0.8 which is equivalent to a pressure loss coefficient of approx. 0.42.

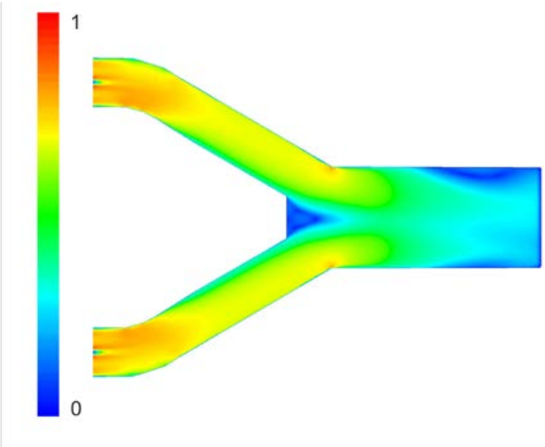

Fig. 18: Velocity magnitudes at plane 1 with inserted perforated plates (GT1 and GT2 in operation)

It can be taken from figure 18 that the flue gas distribution is less homogenous compared to the result presented in figure 16 but considerably better compared with the reference model, and the simulated cases with the baffle plates and the perforated plate cases 1 and 2.

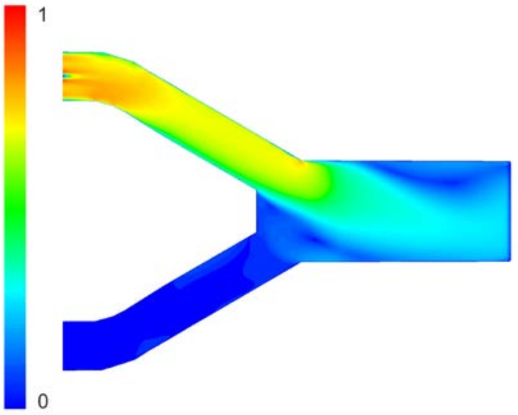

Fig. 19: Velocity magnitudes at plane 1 with inserted perforated plates (only GT1 is in operation)

Fig. 19 represents the velocity distribution of the flue gas in plane 1 for the case that only gas turbine 1 is in operation. The figure shows that also in this case a uneven flow distribution is given. But the fluid structure is similar to that presented in figures 11 and 17 (both calculated with perforated plates with a porosity of 0.65). Based on the higher porosity of the perforated plates with 0.8 at the current test case the vortex area at the left side of the HRSG is a little bit larger compared to the cases 1 and 3 with perforated plates.

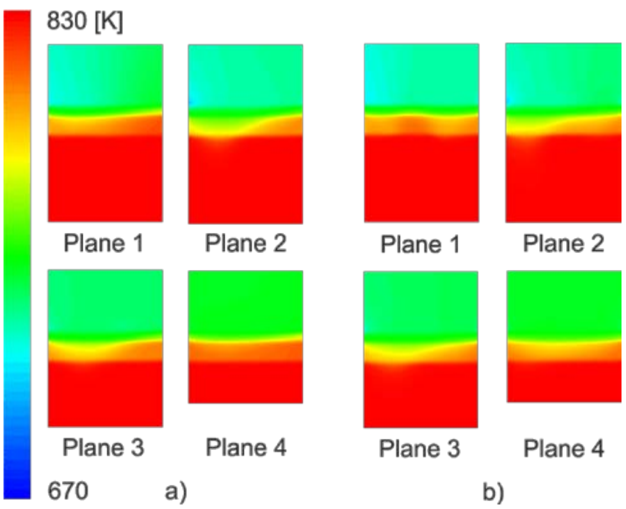

Fig. 20: Vertical temperature distribution of the flue gas (GT1 is in operation) a) perforated plates – case 3 and b) perforated plates – case 4

The temperature distribution of the flue gas in the HRSG is presented in figure 20. Fig. 20a and 20b shows the situation for the case that only gas turbine 1 is in operation.

The figure shows, that in case of a larger channel length between the merging point of the two gas turbine ducts and the entrance into the HRSG results in a more homogenous temperature distribution. This is a result of the more even flue gas distribution in front of the first super heating surface of the HRSG.

5.5 Pressure drop and loss of gas turbine power

As described above is the installation of inserts into a flow channel associated with an additional pressure drop. As mentioned in [15] results an additional pressure loss of 1 mbar in a decrease of the gas turbine efficiency of approx. 0.05% points. Therefore the pressure drop influences the decision for a solution which should be realized in a very strong manner.

TABLE 3

PRESSURE LOSS AND LOSS OF GAS TURBINE POWER

	gas turbines in operation	pressure loss [mbar]	loss of gas turbine efficiency [%]
reference model	2	0.991	-
	1	0.944	-
baffle plates	2	0.958	0.002
	1	1.494	-0.003
perforated plates – case 1	2	5.483	-0.225
	1	4.179	-0.138
perforated plates – case 2	2	2.302	-0.066
	1	2.211	-0.039
perforated plates – case 3	2	5.477	-0.244
	1	2.674	-0.062
perforated plates – case 4	2	1.202	-0.060
	1	0.344	-0.017

Table 3 gives an overview about the additional pressure loss as well as the loss of gas turbine efficiency for the investigated combined cycle power plant. The values included in table 3 for the pressure loss are a result of the calculations with FLUENT and represent the pressure difference between the gas turbine outlet and plane 2 which is arranged in front of the first tube bank SH1. The loss of gas turbine efficiency is calculated from the difference in pressure loss between the referenced model and the models with additional inserts in the channels multiplied with the average efficiency loss factor of 0.05% according to [15].

Based on the higher flue gas mass flow at the operation with both gas turbines the pressure loss is higher compared to the cases with only GT1 in operation.

Table 3 shows also, that the measures with a higher possibility to get a homogenous flow distribution in front of the SH1 have also a higher pressure loss and in last consequence they are linked with a higher loss of gas turbine power respectively a lower efficiency of the combined cycle.

6 Conclusion

In the present investigation a special configuration for a combined cycle power plant are analysed. In this plant two gas turbines are installed to feed one HRSG. The flue gas flow in the channels between the two gas turbines and the HRSG was investigated. The goal of the investigation was to find a channel design to get a homogenous flow distribution in front of the first heating surface of the HRSG which is arranged downstream of the gas turbines. A particular attention was placed in the study at the operation mode with only one gas turbine.

To get a more homogenous flow distribution in front of the first tube bank of the HRSG (entrance of the flue gas into the boiler) the influence of different inserts into the flue gas ducts between gas turbines and HRSG on the flow behaviour are analysed

The results of the study have shown that the measures with a higher possibility to get a homogenous flow distribution in front of the SH1 have also a higher pressure loss and in last consequence they are linked with a higher loss of gas turbine power respectively a lower efficiency of the combined cycle. The study has also shown that a larger merging area for the flue gas arranged upstream of the HRSG results in a more even flow distribution.

For the design engineer it is a question of balance between a more homogenous flow at the entrance of the HRSG and the loss of efficiency of the gas turbine. The study has shown that for such a special arrangement of the power plant no perfect solution can be found to cover all operation modes. Every solution which will be realized depends on the particular boundary conditions which are set by the design engineer or the power plant owner.

7 Acknowledgment

The authors would like to thank BERTSCHenergy, Kessel- und Energietechnik Apparatebau, Josef Bertsch Ges.m.b.H. & Co, Herrengasse 23, A-6700 Bludenz, Austria to make available the boiler and channel data for the present study.

References:

[1] A. Poullikkas, *Introduction to Power Generation Technologies*, New York: Nova Science Publisher, Inc., 2009.

[2] Power plant Emsland (2011, April 18) [Online]. Available: http://www.rwe.com/web/cms/de/16658/rwe-power-ag/standorte/kw-emsland/ (in German).

[3] P. Ratliff, P. Garbett and W. J. Fischer, "The New Siemens Gas Turbine SGT5-8000H for More Customer Benefit", *VGB PowerTech*, vol. 87, pp. 128-132, 2007.

[4] U. Gruschka, B. Janus, J. Meisl, M. Huth and S. Wasif, "ULN System for the new SGT5-8000H Gas Turbine: Design and High Pressure Rig Test Results", in *Proceedings of the ASME Turbo Expo 2008: Power for Land, Sea and Air GT2008*, 9.-13. June, Berlin, Germany, Paper number: GT2008-51208, pp. 1-7, 2008.

[5] M. Huth, U. Gruschka, B. Janus, J. Meisl and S. Wasif, "Design of the Combustion System for the SGT5-8000H and First Experiences in the Irsching Power Plant ", *VGB PowerTech*, vol. 89, pp. 43-47, 2009.

[6] W. J. Fischer, "SGT5-8000H Product Validation and Operational Experience at Irsching 4", in *Proceedings of the PowerGen Europe 2010*, 8.-10. June, Amsterdam, Netherlands, pp. 1-15, 2010.

[7] H. Walter,"Reverse Flow in Natural Circulation Systems with Unequally Heated Tubes", *WSEAS TRANSACTIONS on HEAT and MASS TRANSFER*, vol. 1, pp. 3-10, 2006.

[8] H. Walter, "Theoretical Stability Analysis of a Natural Circulation Two-Pass Steam Generator: Influence of the Heating Profile and Operation Pressure", *WSEAS TRANSACTIONS on HEAT and MASS TRANSFER*, vol. 1, No.: 3, pp. 274-282, 2006.

[9] H. Walter and W. Linzer, ”Flow Stability of Heat Recovery Steam Generators”, *ASME Journal of Engineering for Gas Turbines and Power*, vol. 128, pp. 840-848, 2006.

[10] H. Walter and W. Linzer, ”Investigation of the stability of a natural circulation two-pass boiler”, *Heat and Mass Transfer*, vol. 42, No.: 6, pp. 562-568, 2006.

[11] H. Walter, “Numerical Stability Analysis of a Natural Circulation Steam Generator with a Non-uniform Heating Profile over the tube length”, in *Proceedings of the 4th IASME / WSEAS Int. Conf. on HEAT TRANSFER, THERMAL ENGINEERING and ENVIRON-MENT*, 21.-23. August, Elounda, Agios Nikolaos, Crete Island, 2006

[12] BERTSCHenergy, Combined Cycle and Cogeneration HRSG. Josef Bertsch GmbH & Co. KG, Bludenz, 2010.

[13] Fluent, *Fluent 6.3 User's manual*. Fluent Inc., Lebanon, NH, USA, 2006.

[14] S.V. Patankar, *Numerical heat transfer and fluid flow*, Series in Computational Methods in Mechanics and Thermal Sciences. Hemisphere Publ. Corp., Washington, New York, London, 1980.

[15] R. Dolezal, *Combined gas- and steam power plants*, Springer Verlag, Berlin, Heidelberg, New York, 2001 (in German).

[16] W. Zhou, A. Marquez, D. Moyeda, S. Nareddy, J. Frato, G. Yu, S. Knarvik and V. Frøseth, “Design and Test of a Selective Noncatalytic Reduction (SNCR) System for Full-Scale Refinery CO Boilers To Achieve High NOx Removal“, *Energy & Fuels*, vol. 24, pp. 3936-3941, 2010.

[17] T. Le Bris, F. Cadavid, S. Caillat, S. Pietrzyk, J. Blondin and B. Baudoin, “Coal combustion modelling of large power plant, for NOx abatement“, *Fuel*, vol. 86, pp. 2213-2220, 2007.

[18] C. R. Choi and C. N. Kim, “Numerical investigation on the flow, combustion and NOx emission characteristics in a 500 MW_e tangentially fired pulverized-coal boiler“, *Fuel*, vol. 88, pp. 1720-1731, 2009.

[19] S. Belosevic, M. Sijercic, S. Oka and D. Tucakovic, “Three-dimensional modeling of utility boiler pulverized coal tangentially fired furnace” *International Journal of Heat and Mass Transfer*, vol. 49, pp. 3371-3378, 2006.

[20] E. Fried and I. E. Idelchik, *Flow Resistance: A Design Guide for Engineers*, New York, Washington: Hemisphere Publishing Corporation, 1989.